ADVANCED ELECTRONIC MATERIALS
Open Access

Supporting Information

for *Adv. Electron. Mater.*, DOI 10.1002/aelm.202300520

Correlation between Electronic Structure, Microstructure, and Switching Mode in Valence Change Mechanism Al_2O_3/TiO_x-Based Memristive Devices

*Stephan Aussen, Felix Cüppers, Carsten Funck, Janghyun Jo, Stephan Werner, Christoph Pratsch, Stephan Menzel, Regina Dittmann, Rafal Dunin-Borkowski, Rainer Waser and Susanne Hoffmann-Eifert**

Supplementary Information for the manuscript

Correlation between Electronic Structure, Microstructure and Switching Mode in Valence Change Mechanism Al_2O_3/TiO_x-based Memristive Devices

Stephan Aussen, Felix Cüppers, Carsten Funck, Janghyun Jo, Stephan Werner, Christoph Pratsch, Stephan Menzel, Regina Dittmann, Rafal Dunin-Borkowski, Rainer Waser and Susanne Hoffmann-Eifert**

S. Aussen. Dr. F. Cüppers, Dr. C. Funck, Dr. S. Menzel, Prof. Dr. R. Dittmann, Prof. Dr. R. Waser, Dr. S. Hoffmann-Eifert
Peter Grünberg Institut (PGI 7 and 10) and JARA-FIT, Forschungszentrum Jülich GmbH, Wilhelm-Johnen-Straße, 52428 Jülich, Germany
E-mail: s.aussen@fz-juelich.de; su.hoffmann@fz-juelich.de

Dr. S. Werner, Dr. C. Pratsch
Helmholtz-Zentrum für Materialien und Energie GmbH, Department X-ray Microscopy, Albert-Einstein-Str. 15, 12489 Berlin, Germany

Dr. J. Jo, Prof. Dr. R. Dunin-Borkowski
Ernst Ruska-Center (ERC-1 / PGI-5) and JARA-FIT, Forschungszentrum Jülich GmbH, Wilhelm-Johnen-Straße, 52428 Jülich, Germany

S. Aussen
RWTH Aachen University, Templergraben 55, 52062 Aachen, Germany

Prof. Dr. R. Waser
Institute of Materials in Electrical Engineering and Information Technology II, RWTH Aachen University, Sommerfeldstraße 24, 52074 Aachen, Germany

1. Area-dependent switching mode

Retention behavior of the a-HRS and a-LRS

To verify the non-volatile memristive character of the area-dependent switching mode in Pt/1.2 nm Al_2O_3/7 nm TiO_x/Cr/Pt, a state retention measurement was performed on the two resistive states *a*-HRS and *a*-LRS. For this, a 60 nm × 60 nm device was initialized by switching at least 50 times. Subsequently, the *a*-HRS state was programmed by applying a voltage sweep of 1 V/s with a maximum voltage of -2.0 V to the active Pt electrode. The device was read at room temperature in the given time steps by a sweep signal up to -500 mV. The resistance was calculated at this voltage and is shown as open symbols in Figure S1. The measurement was stopped after 26 hours. After programming the *a*-LRS by applying +2.0 V to the active Pt electrode, the same reading procedure was repeated up to 17 hours. The results are shown as closed symbols in Figure S1.
The stable states' retention indicate that the switching is a permanent resistance change and nonvolatile.

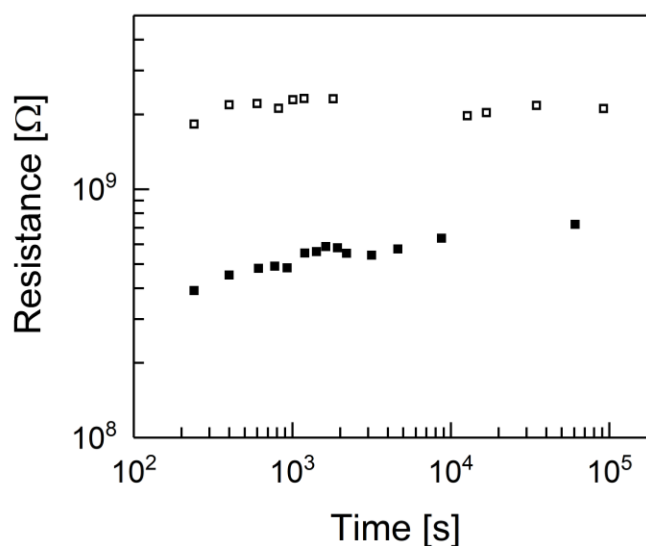

Figure S1. Retention measurements of the area-dependent states of a $(60\ \text{nm})^2$ device. *a*-HRS is shown as open symbols and *a*-LRS as closed symbols.

Switching stability of the area-dependent mode

Furthermore, the switching stability of the area-dependent mode was tested. For this, a previously initialized Pt/1.2 nm Al_2O_3/7 nm TiO_x/Cr/Pt device of 300 nm × 300 nm size was repeatedly switched with voltages of +2.3 V for SET and -2.3 V for RESET at room temperature. The voltage ramp was kept at a low value of 0.3 V/s to follow-up with the slow switching kinetics of the device. The *a*-HRS and *a*-LRS resistances were calculated at -500 mV for each *I*-*V* curve. The results are shown in Figure S2. When the measurement was concluded after 300 switching cycles, the device was still operable in the typical behavior.
The stable endurance over several hundred switching cycles demonstrates the reproducibility of the switching process.

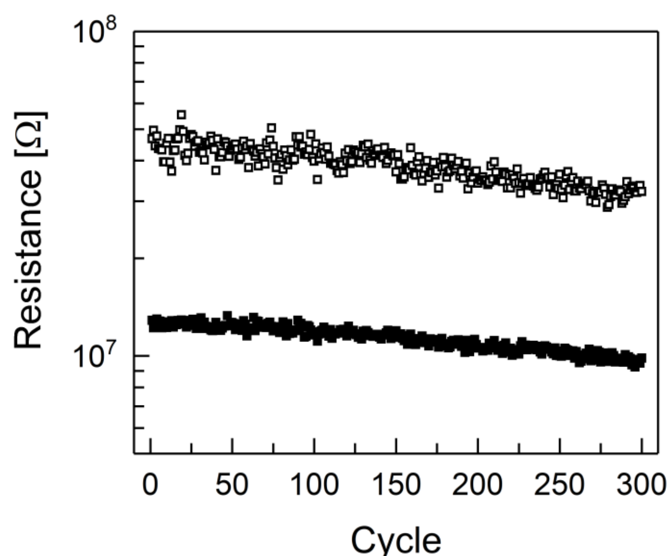

Figure S2. Endurance measurement of the area-dependent switching of a (300 nm)^2 device. *a*-HRS is shown as open symbols and *a*-LRS as closed symbols.

2. Spectroscopic investigations

Devices switched in the filamentary mode

To further illustrate the local structural and chemical changes in the filamentary switched device, which is discussed in Figure 4 of the publication, Figure S3 shows the principal component analysis (PCA) of a larger area around the filament that is marked by a white arrow. The PCA allows the identification of changes not only inside but also outside the device area. The contrast in Figure S3 a) correlates to the different materials and thicknesses of the micro-crossbar device showing the cross-junction device area as the darkest region due to the strongest absorption. In Figure S3 b) the filamentary region corresponding to reduced TiO_{2-x} appears as a dark spot in the lower right corner of the device area. In addition, TiO_x material that remained after etching of the TE due to non-ideal vertical side walls is seen as a bright vertical line at the left side of the vertical TE. Therefore, the component representing the map in Fig. S3 b) is attributed to amorphous TiO_x. There is another Ti L-edge component which is mapped in Figure S3 c). For this component, the filament appears black, which equals low intensity, whereas a circular-shaped region around the filament appears bright. The structure and chemical composition of the titanium oxide in this halo (H) region is different form reduced TiO_{2-x} and from amorphous TiO_x. The component extends centrosymmetric around the filament. Analysis of a reference spectrum shown in Figure 4 f) indicates that the component relates to rutile-type TiO_2. The intensity is higher outside the device area due to the missing absorption by the Pt TE.

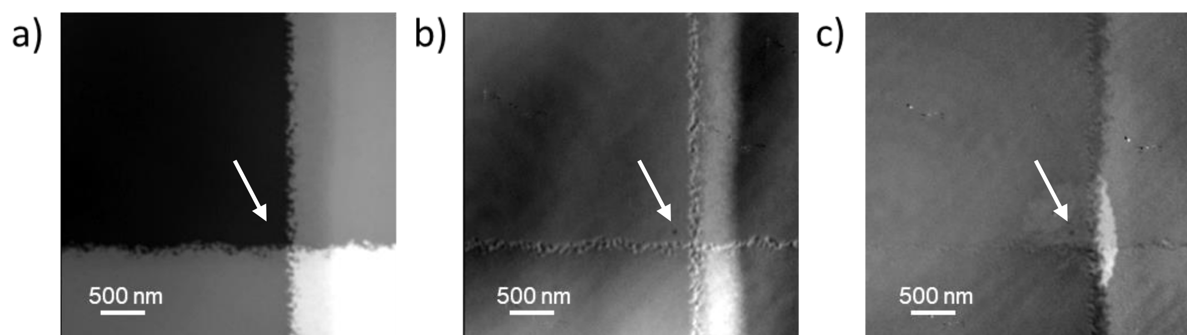

Figure S3. a)-c) Component maps at the Ti L-edge enabling the identification of regions of amorphous TiO_x (device), reduced TiO_{2-x} (filament) and rutile-type TiO_2 (halo).